



Geochemical characteristics of rehabilitated tailings and associated seepages at Kidston gold mine, Queensland, Australia

Mansour Edraki^a , Thomas Baumgartl^a , David Mulligan^a, Warwick Fegan^a
and Ali Munawar^b

^aCentre for Mined Land Rehabilitation, Sustainable Minerals Institute, The University of Queensland, Brisbane, Australia; ^bFaculty of Agriculture, University of Bengkulu, Bengkulu, Indonesia

ABSTRACT

This study investigated an uncapped tailings storage facility in a semi-arid subtropical climate, with the aim of understanding the hydro-geochemical processes controlling the seepage water quality and the dispersion/attenuation of metals and metalloids within the tailings and through a constructed wetland. While direct re-vegetation helped to stabilize the surface of tailings, development of an oxidation front in the tailings resulted in high sulphate and arsenic concentrations in the seepage. The findings of this study will assist maximizing the efficiency of any future passive treatment system on site and provide useful information for similar tailings closure strategies elsewhere.

ARTICLE HISTORY

Received 26 April 2016
Accepted 29 July 2017

KEYWORDS

Tailings; rehabilitation; water quality; mine closure

Introduction

In some environments where suitable capping materials and growth media for vegetation are scarce, an optional potential strategy for managing water in decommissioned tailings storage facilities (TSFs) is direct revegetation of tailings, although there are very few published examples of such an approach [1,2]. The establishment of vegetation directly into tailings can be used to physically stabilise the tailings surface to prevent erosion and dust generation, encourage soil biological processes and reduce deep infiltration of rainwater through the process of evapotranspiration. Tailings pore water, however, may continue to retain high concentrations of sulphate and other constituents for some time depending on the rate of geochemical processes within tailings. Salmon and Malström [3], for example, have described the weathering of aluminosilicate minerals, oxidation of sulphide minerals by both dissolved molecular O₂ and Fe(III) and oxidation of aqueous Fe(II) as slow kinetically controlled processes, and aqueous speciation, Henry's law equilibrium between aqueous solution and tailings pore gases, and dissolution/precipitation of secondary minerals as fast equilibrium-controlled processes in tailings.

Detailed geochemical studies of uncapped metallic tailings have previously focused on relatively old TSFs with deep weathering zones such as Chilean [4,5] or Canadian examples [6]. There have been also recent attempts to study oxidation processes in fresh tailings [7]. Other detailed geochemical studies of tailings (in Sweden) have focused on modelling the geochemical processes occurring in the unsaturated zone of carbonate-depleted pyritic tailings deposits [3], remediated tailings [8] or flooded tailings [9]. There are published Australian examples of covered tailings [10,11] and uncapped tailings in abandoned or legacy sites inherited from inadequately regulated past mining practices [12].

This current study characterised the tailings materials, groundwater and seepage, 10 years after an uncapped TSF was closed with the aim to (1) describe better the tailings weathering and its impact on seepage water quality, and (2) investigate the function of a wetland which was constructed to improve the seepage water quality. Such investigations provide an opportunity to follow the geochemical processes in tailings in conjunction with the rehabilitation monitoring programme. The outcomes from this study will help to better understand the weathering and oxidation processes and discharge of poor quality seepage water, and hence lead to better management strategies for TSFs in similar semi-arid climates.

Site setting

Kidston is a closed gold mine in the semi-arid sub-tropical region of northern Australia (Figure 1) with average annual rainfall of around 700 mm and fourfold higher pan evaporation. Gold mineralisation at Kidston was hosted by a breccia pipe with fragments of granodiorite, felsites, quartz-feldspar porphyry and local metamorphic [13]. Alluvial gold recoveries at Kidston began in the late nineteenth century and there were periods of small-scale hard rock mining in the first half of the twentieth century. However, the main large-scale open-pit mining operation at Kidston started in 1985 and finished in 2001. During this time, about 3.5 million ounces of gold was produced [14] through cyanide leaching, carbon in-pulp and carbon column technology followed by carbon stripping, electrowinning and smelting.

The TSF at Kidston is a roughly triangular shape (Figure 1) engineered dam covering an area of about 310 ha with constructed walls on two sides and a natural hill forming the third boundary. During its lifetime, the tailings dam wall was progressively raised with five lifts to the outer wall using competent rock for structural strength and a compacted impermeable zone on the inside of the wall [15]. The walls of the dam were designed to leak to prevent wall failure due to high pore pressures [16]. Wet tailings (45% solids) were discharged from spigots adjacent to the dam walls. Tailings deposition ceased in 1997 and the TSF was successively rehabilitated by seeding and planting of native trees, shrubs and a mix of native and introduced pasture grasses from 1998 to 2001. The revegetation of the uncapped tailings was typically achieved through a combination of supplemental irrigation, fertilisation and phased planting and seeding to try to allow sufficient tree and shrub establishment prior to the introduction of grasses. Transect-based measurements of local native vegetation communities determined that a target of 70% effective ground cover would provide evidence of effective rehabilitation. The majority of the monitored tailings surface reached or were close to these nominal targets within a few years of seeding.

The waste rocks were truck dumped in surface engineered dumps surrounding the open pits. The sub-economic mineralised waste rocks, for example the south dump which was close to the TSF, were potentially acid forming and were capped on the top with an engineered cover [17].

The wetland shown in Figures 1 and 2 was constructed with oxide rock overlying a coarse rock layer (Figure 3) with earth berms arranged in a maze form to hold and direct water flow and provide enough residence time for reactions to happen. The wetland had reeds in the furrows and trees grown on the ridges.

Materials and methods

In 2007, following a reconnaissance survey of the TSF by manual auguring at several locations to a depth of 6 m, which consistently showed the presence of a grey un-oxidised layer at a depth of ~1.5–2 m, a number of trenches were dug and samples collected from vertical sections at several intervals to cover a variety of horizons. The deepest sample from each section was collected with an auger from the un-oxidised zone. Samples were subjected to total digest analysis. For major oxides, samples (0.15 g), standard reference materials and procedural blanks were fused with lithium metaborate (Sigma–Aldrich, 1:4 sample/flux) in graphite crucibles (Alpha Resources, USA) at 1000 °C for

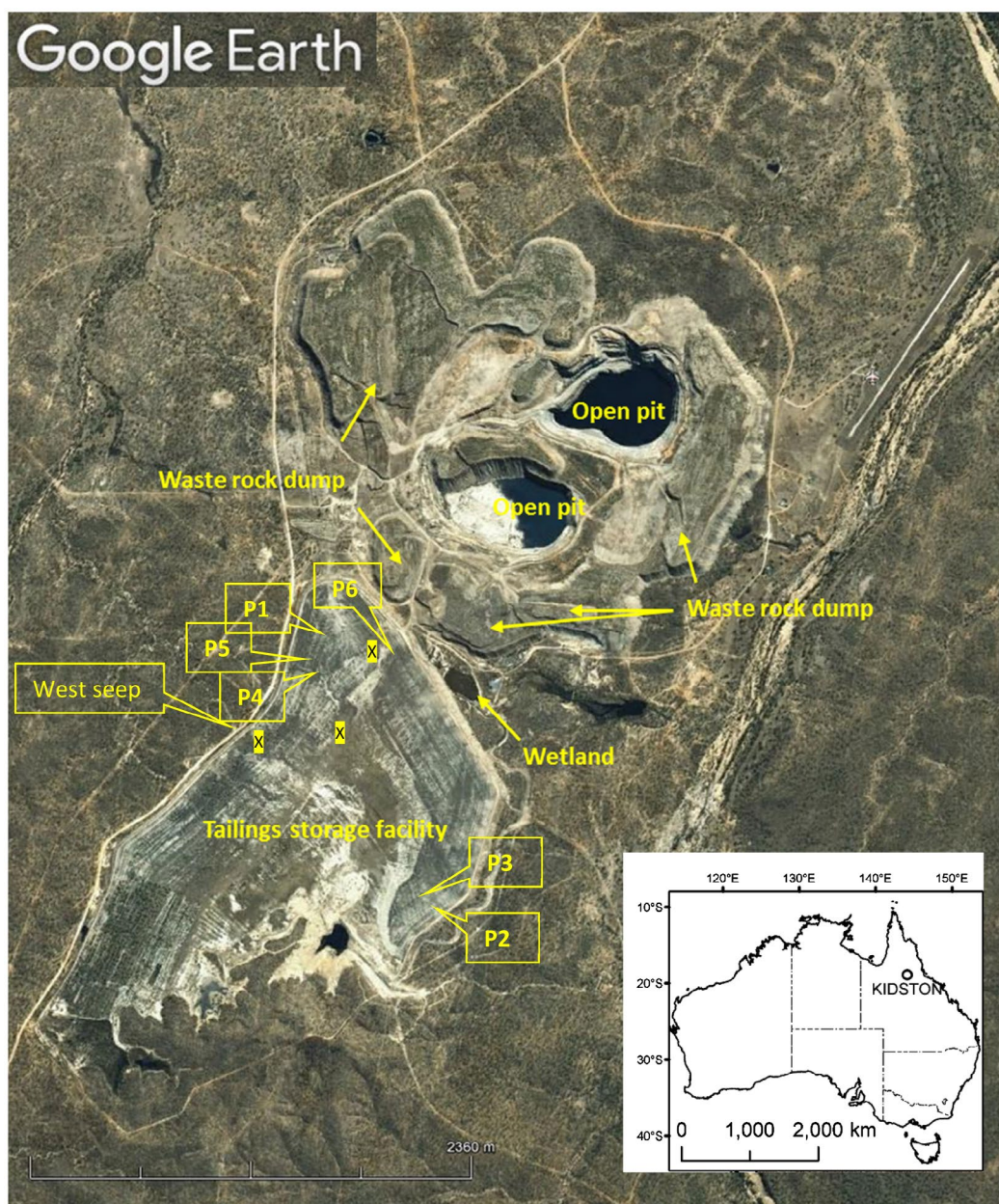


Figure 1. Kidston mine location and site lay out; P1–P6 = piezometers; X = trench.

1 h. The samples were then dissolved in 10% HNO_3 and diluted by Milli-Q water to a sample/solid weight ratio of 1: ~1000. Lutetium was added as internal standard. Major elements were measured using a Perkin Elmer Optima 3300 DV optical emission spectrometer based on the principles of US-EPA Method 6010B. For trace elements, ~100 mg of sample was dissolved using concentrated HNO_3 -HF mixtures (1:3) at 150 °C in screw-capped Savillex PFA beakers. Following digestion the samples were evaporated to incipient dryness and the sample cake digested in 6 M HNO_3 overnight. The contents were then evaporated to incipient dryness again and re-dissolved in 2 mL of concentrated HNO_3 . Final sample preparation was undertaken, following addition of known weights of internal standard

(Rh, In, Re) solution, by dilution with Milli-Q water to a sample/solution weight ratio of 1: ~100,000. Trace metal concentrations were determined on a Thermo Electron X-7 series ICP-MS.

A sequential extraction procedure [18] was applied to selected tailings samples. Solid samples were air dried. One gram of <5 µm powder was placed into a 50-mL centrifuge tube and dissolved sequentially in different reagents. The four step extraction included (1) the water-soluble fraction with deionised water, (2) the carbonate and exchangeable fraction with 1 M NH_4 -acetate solution buffered at pH 4.5, (3) metals bound to amorphous and poorly crystalline Fe-phases with 0.5 M NH_4 -oxalate solution and (4) elements co-precipitated with well crystalline phases of Fe such as goethite (FeOOH) and jarosite ($\text{KFe}_3(\text{SO}_4)_2(\text{OH})_6$) with 1 M $\text{NH}_2\text{OH} \cdot \text{HCl}$ solution in 25 vol.% acetic acid at <96 °C.

The mineral identification of all solid materials was made by a Bruker D8 Advance X-ray diffractometer equipped with a Cu target, diffracted-beam monochromator and scintillation counter detector. Conditions for running the samples were 40 kV, 30 mA, 3–80 2θ , 0.05° step size or increment, with 10 s per step. Software used for mineral identification was DIFFRAC^{plus} Evaluation Search/Match Version 8.0.

At least 50 mL of water samples were filtered (0.45 µm) in the field and preserved with HNO_3 at pH < 1 for metals analysis (except for ferrous iron which was preserved with HCl) by ICP-OES and ICPMS depending on the concentration. All samples, including 500 mL of unfiltered samples for alkalinity, major cations and anions measurements, were transported and stored at below 4 °C until analysed. Secondary minerals, flocculants and efflorescence salts collected around a wetland area that had been constructed by the mine to manage some of the seepage, were dissolved in hot aqua regia ($\text{HCl} + \text{HNO}_3$) and analysed by ICP-MS. Collected plant leaves from the wetland were dried, ground, digested using a 5 HNO_3 :1 HClO_4 acid mix and analysed.

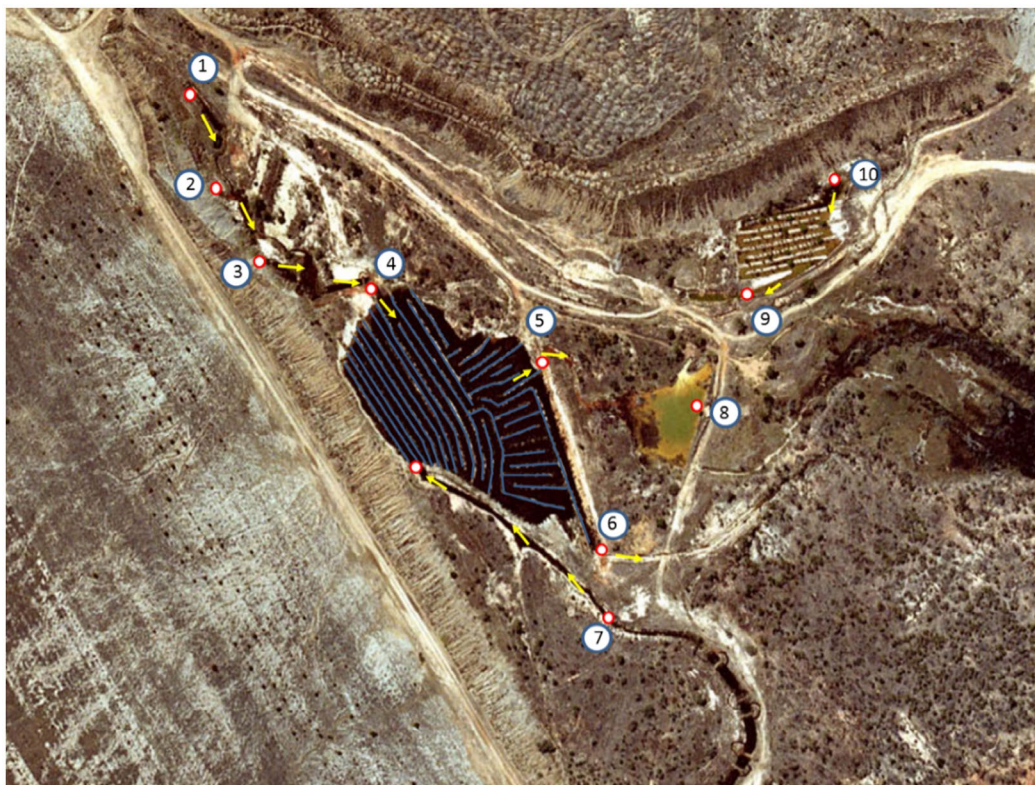


Figure 2. The wetland maze area and sample locations: P1–P6 = Piezometers; 1 = Seep1; 2 = Seep2; 3 = Seep3; 4 = Maze Inflow 1; 5 = Maze outflow; 6 = Maze overflow; 7 = Maze inflow2; 8 = Reclaim pond; 9 = WRD pond outflow; 10 = WRD seep source. Arrows show direction of water flow.

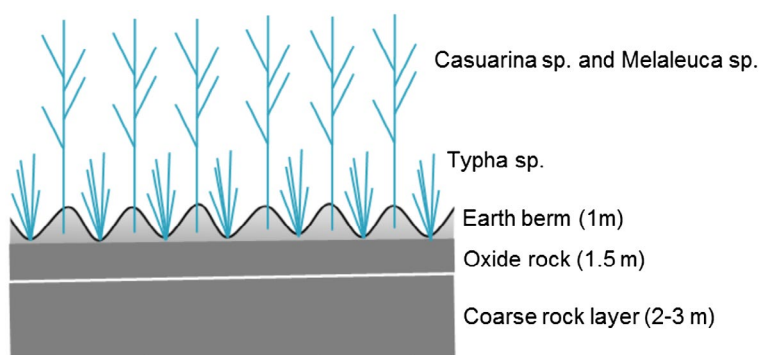


Figure 3. Cross section of the constructed wetland.

Results and discussion

Tailings mineralogy and geochemistry

The mineralogy of tailings samples studied reflects the ore breccia lithologies that were dominated by quartz, plagioclase, chlorite, biotite, amphibole, muscovite, calcite and magnetite, with weathering products such as hematite and ankerite, gypsum and various degrees of alteration products (clay etc.), also present. The results also showed evidence of oxidation before and after ore processing. Pyrite was the most abundant sulphide present followed by arsenopyrite and chalcopyrite.

According to Roseby et al [19] the unoxidised (fresh) tailings sampled in 1994 during the operation had an alkaline pH (7.2–8.9) with a median of 8.1. The unoxidised EC values ranged from 0.19 to 4.05 dS/m with a median of 0.81 dS/m. Total S ranged from 0.6 to 4.2% (median = 1.3%) and the acid/base accounting demonstrated that the majority of the tailings material will not be net acid generating [19]. The tailings samples of the current study were mostly neutral to alkaline (up to pH 8), with some layers showing acidic pH values (pH 3–4). Electrical conductivities were in the range of 0.2–4.8 dS/m.

The trench profiles showed distinctive layering particularly in the central parts of the TSF due to the sedimentary processes such as graded bedding by grain size and weight difference, and also different mineralogy during deposition. The median particle size (D_{50}) of the whole tailings is about 0.05 mm [20]. The tailings are about 51% silt-sized, 47% sand sized and 2% clay-sized. They can be described as sandy silt. The coarser grain tailings with higher sulphide percentage were located closer to the former discharge points near the TSF walls. The upper part of the tailings or the oxidised zone with white, red and orange colour overlies a distinct grey moist and apparently unoxidised zone at about 1.5–2-m profile depth. The depth of the oxidised zone, which is deeper closer to the TSF walls, had deepened in recent years compared to what was previously reported (0.4 m). Grey tailings also appeared as thin horizons and lenses in the oxidised zone.

Based on geology records [21], sulphides had been weathered to an average depth of 30 m throughout the orebody. The upper half of the oxidation profile was stained by a red-brown colour due to goethite and hematite after oxidation of pyrite and pyrrhotite. Microscopic textural features such as extensive iron oxidation around original crystal grains were used as evidence of tailings minerals oxidation prior to the deposition. Table 1 shows the range of chemical composition of tailings samples collected from the trench profiles. Despite the less oxidised nature of the grey zone, the bulk elemental/mineral composition of the two zones, at least for the range of samples analysed, is not significantly different. This is due to uncompleted oxidation processes or slow kinetic reactions in the oxidised zone. However, there was a distinct variation in the degree of oxidation and tailings chemistry, based on the texture of various horizons, with more obvious oxidation of finer horizons which had higher water retention capacity. For example, at 56–60-cm depth in a trench in the middle of the TSF (TR7, Figure 4) which showed more obvious features of oxidation, there was higher Fe, As, Mo, P and S and

Table 1. The median and range of tailings composition (*n* = 13).

Major oxides (Wt%)		Minor and trace elements (mg/kg)			
SiO ₂	65.46 (51.70–69.36)	As	125 (14.60–605)	Pb	281 (13.2–464)
Al ₂ O ₃	13.76 (11.98–16.23)	Ba	4035 (196–5056)	Rb	162 (57–221)
CaO	2.12 (1.34–3.71)	Be	2.49 (1.07–2.80)	Sb	6.26 (1.84–15.8)
Fe ₂ O _{3T}	5.77 (3.76–8.29)	Cd	47.87 (0.43–10)	Sn	10.26 (0.42–22.4)
K ₂ O	2.75 (2.15–4.55)	Co	11.96 (2.32–29.20)	Sr	317 (191–447)
MgO	1.45 (0.36–1.91)	Cr	8.55 (2.71–39.1)	U	1.59 (0.36–2.12)
MnO	0.13 (0.015–0.232)	Cu	171 (29.2–289)	V	79.2 (47.5–114)
Na ₂ O	2.19 (1.32–2.98)	La	23.11 (6.05–32)	W	10.31 (10.3–17.7)
P ₂ O ₅	0.090 (0.059–0.205)	Li	17.5 (6.9–51.1)	Zn	1424 (35–4359)
TiO ₂	0.48 (0.34–0.57)	Mo	8.88 (2.86–36)	Zr	91.11 (39.3–118)
		Ni	25 (3.37–42.9)	S	1.74 (1.00–2.93)

TR2-
Fine grained (0.1-0.5mm),
Qtz, Pyr(2%), Asp(<0.5%),
Chl, Cal (2-5%), little-minor
post deposition oxidation

TR7-
Fine grained (<0.01 -
0.5mm), remnant
granodiorite textures, strong
oxidation of Pyr and Asp,
abundant Fe oxides

TR10-
Very fine grained (<0.1mm)
rich in Cal (up to 10%) , Fe
oxides, Pyr (2-5%), intense
oxidation

TR13-
Very fine grained (average
size <0.05mm), patchy
oxidation, upper part of the
“unoxidised” zone

TR14-
Coarse grained (<0.01mm to
0.7mm), intact grains of Asp
present (0.2-0.4mm) –
negligible post-deposition
weathering, Pyr (~1%)

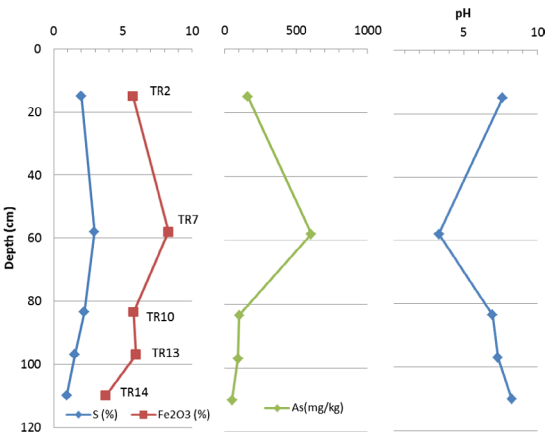


Figure 4. A comparison of microscopic observations, field profiles and tailings chemistry; Qtz = quartz, Asp = arsenopyrite, Pyr = pyrite, Chl = chlorite, Cal = calcite.

lower Sr, Ba, Ce, Mn, La, Pr, Nd, Sm, Eu, Sc and Co. This horizon had lower pH (3.31) and a heavier (clay) texture with a moisture content of 24.5%. On the other hand, remnant fresh arsenopyrite and pyrite grains were not uncommon in the coarse-grained tailings near the TSF wall with less water retention capacity where the oxidation products are leached down and to some extent retained by forming a hardpan layer at a depth of about 1 m.

After high intensity rainfall events, with little infiltration to deeper depths, the moisture remains closer to the surface and rises by evaporative forces in fine-grained tailings resulting in the accumulation of metal-enriched salts near the tailings surface. The effect of upward water fluxes was more pronounced in the central tailings area with accumulation of salt crusts during the dry months. A geochemical survey of the surface of the TSF at 100 m × 300 m grid intervals in 2007 showed relatively enriched, but still trace (<100 mg/kg), quantities of Cd in a number of surface samples collected from the central area of the TSF at a depth of 0–10 cm. The survey also found the presence of trace (<100 mg/kg) to elevated (>100 mg/kg) quantities of Pb, Zn, Cu and As, in a decreasing order of concentration, respectively. Main salt minerals present were gypsum (CaSO₄·2H₂O), halite (NaCl), ankerite [Ca(Fe⁺²,Mg)(CO₃)₂] and epsomite (MgSO₄·7H₂O).

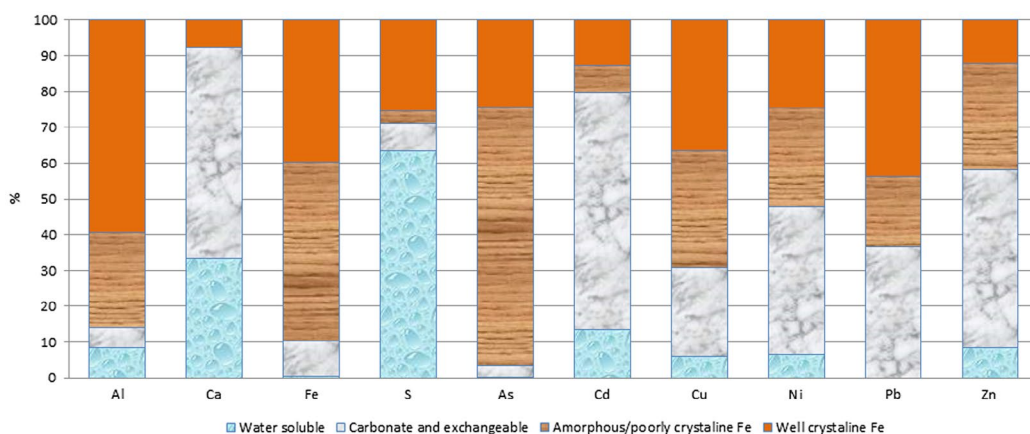


Figure 5. Percentages of major and trace elements in four geochemical fractions of selected tailings samples (average of 6 samples).

Notwithstanding the observations of temporary surface accumulation, however, in the wet–dry climate of northern Australia, unlike, for example, the hyper-arid areas of northern Chile [4], the dominant long-term direction of metals transport in the TSF is downward. In addition to rainfall intensity and grain size of tailings, the preferential flow paths and structure of the pores are also important factors in water movement throughout the tailings. For example, horizontal hydraulic conductivity measured at a depth of 20 cm in a trench in the central area of the TSF was 4.4×10^{-3} cm/s compared to 8.7×10^{-5} cm/s for vertical direction. Furthermore, in the case of samples collected at different depths, the average hydraulic conductivity measured on repacked samples, which did not simulate field conditions (e.g. the grain structure of tailings), was >360 times greater than the undisturbed measurements. The same test showed an increase by a factor of only 1.6 for samples collected from the same horizon.

The results of sequential extraction tests, which focused on secondary minerals, to some degree reflected the mode of occurrence of elements in various horizons of the profile, depending on the mineralogy and degree of oxidation. Arsenic and iron were mainly associated with amorphous/ poorly crystalline Fe phases (Figure 5), particularly in horizons which had been highly oxidised (e.g. TR7, Figure 4). Cadmium, although predominately in the exchangeable phase, was in water soluble form in TR7 along with Mn and Zn, indicating the sequestration of these elements by soluble salts. The water-soluble fraction also contained considerable amounts of S, Na, Ca and Mg (e.g. TR2 and TR7) that could be attributed to the presence of sulphate hydrate minerals. Aluminium was mainly associated with well crystalline Fe phases.

Piezometric levels and water chemistry in TSF

The freshly deposited tailings contained an aquifer system maintained by TSF walls which were designed to leak tailings water into a surrounding system of interception drains. Tailings deposition within the TSF ceased in August 1997. Between 2001 and 2006, the water levels in the piezometers dropped on average between 3 and 5 m, ca. 2.5 m of which could be attributed to an equivalent lowering of the overflow created by the opening of a spillway in 2002.

Seasonal effects of TSF groundwater levels, which could not be detected in the early years due to the continuous fall in the phreatic surface, have been recognised since 2005. More recently (2008–2009), the water levels have returned to the 2003 levels (Figure 6). As rain events are generally heavy, it can be assumed that gravitational water flow in the tailings pore system will occur at close to saturation conditions. However, despite the high infiltration rate into the tailings it seems that the travel time of water towards the phreatic zone is slowed down by layers of tailings sediments with significantly lower

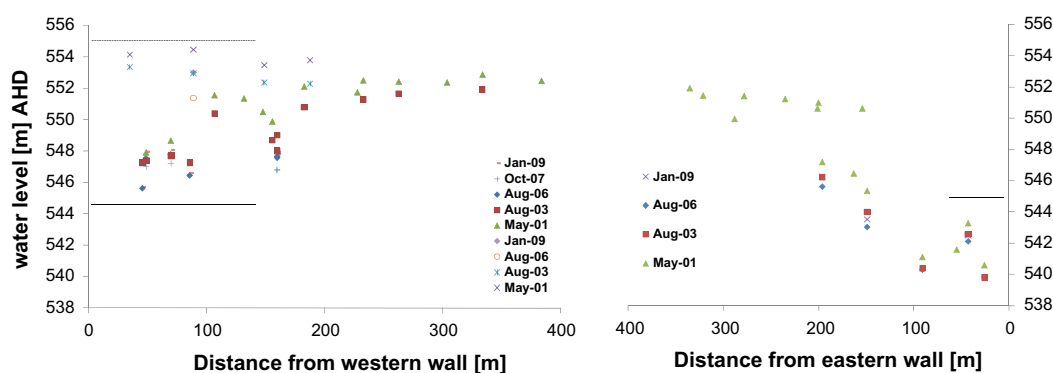


Figure 6. Water levels in the piezometers. Horizontal lines show the base of the dam wall. The constructed wetland is at 534 m level.

hydraulic permeabilities. A dome-shaped aquifer can be inferred from the piezometer measurements with levels lower along the perimeter of the TSF (particularly near the seepage points) compared to the centre.

The groundwater level in the TSF is substantially lower along the eastern wall where much higher seepage flow rates have been recorded. The tailings seepages, reduced to 1–2 L/S in 2005 because of below-average rainfall, have increased to 3–5 L/S recently, but are still much lower than those measured in 1998 (7–8 L/S). There is a general trend of decreasing water levels towards the east and around the western seepage. Considering the underlying topography [22], it is likely that water will preferentially drain towards the east. The potential for deep groundwater leakage from the tailings impoundment is limited because of the relatively impervious nature of the base geology.

Table 2 summarises the water chemistry of samples collected in this study. The groundwater samples from the TSF showed slightly acidic to alkaline pH values (6.1–7.7) and a range of conductivities (5600–10000 $\mu\text{S}/\text{cm}$) and alkalinities (12–460 mg/L). The particularly high bicarbonate alkalinity was the result of carbonates present in the tailings. The concentration ranges of major cations and anions in the sampled groundwater from the TSF were 320–1500 mg/L Na, 67–430 mg/L Ca, 24–69 mg/L Mg, 12–97 mg/L K, 720–3900 mg/L SO_4 and 93–900 mg/L Cl.

Piezometers located in the western part of the TSF contained Na- SO_4 type waters while one sample from the eastern piezometers was predominantly Na-Cl type (B7, Figure 7). High concentration of Na could be related to the use of sodium cyanide in mineral processing, although the authors could not verify that. Only one piezometer had a detectable ferrous iron (1.7 mg/L) concentration which supports the general oxidising conditions at shallow depths of sampling near the water table.

Concentrations of up to 2.1 mg/L Fe, 0.05 mg/L Cu, 0.62 mg/L Zn, 0.300 mg/L Co, 0.09 mg/L Mo, 0.12 mg/L Al, 0.68 mg/L As, 0.0024 mg/L Cd, 0.002 Pb and 0.004 mg/L Sb were detected, while concentrations of Cr, Ni, Hg, Se and Li were all below detection limits.

The results of Saturation Index (SI) calculations using PHREEQC code [23] with the WATEQ4F database [24] showed that the phases likely to be controlling aqueous concentrations of Cu, Pb, Cd, Zn and As, as suggested by Nordstrom and Alpers [25], are undersaturated in the tailings-entrained water except for $\text{Ba}_3(\text{AsO}_4)_2$. A range of redox potentials were tested and similar results were obtained. Gypsum [$\text{CaSO}_4 \cdot 2\text{H}_2\text{O}$, anhydrite (CaSO_4)] and amorphous $\text{Al}(\text{OH})_3$ were, however, close to equilibrium although still unsaturated. The groundwater samples were supersaturated with respect to Alunite [$\text{KAl}_3(\text{SO}_4)_2(\text{OH})_6$] and barite (BaSO_4). This indicates that once heavy metals are dissolved, they are unlikely to be attenuated at the lower depths of the tailings.

Table 2. Chemistry of tailings water in piezometers, seepage water, and surface water around wetland system.

	Piezometers			West Seep	Seep1	Seep2	Seep3	Maze inflow1	Maze inflow2	Maze Outflow	Maze Overflow	WRD Seep Source	WRD Pond Outflow	Reclaim Pond
	Range	Mean	Median											
pH	6.1–7.7	7.1	7.2	7.5	7.6	7.2	5.7	7.5	7.5	6.8	7.5	4.2	4.2	7.7
Electrical Conductivity ($\mu\text{S}/\text{cm}$)	5600–10000	7800	7650	10000	4900	5100	5900	5100	5600	5600	5400	5700	6200	5900
Total dissolved Solids (mg/L)	3000–6300	4400	4250	6300	9400	4100	5300	4200	4200	4700	4500	6400	7300	5000
Total Alkalinity (mg/L)	12–460	116	49	180	230	140	17	160	130	290	180	<5	<5	250
<i>Major cations and anions (mg/L)</i>														
SO ₄	720–3900	2270	2500	3600	1700	1900	2700	2200	2100	2400	2300	3400	3700	2700
Cl	93–900	347	270	190	160	190	180	190	130	220	190	70	74	210
Na	320–1500	800	770	1200	650	610	720	680	630	790	740	450	520	770
K	12–97	52	56	67	76	120	92	100	99	97	100	10	10	92
Ca	67–430	308	365	590	290	360	460	330	390	400	380	460	530	420
Mg	24–69	39	32	120	87	55	150	75	76	90	90	420	500	130
<i>Minor and trace elements ($\mu\text{g}/\text{L}$)</i>														
Fe	<50–2100	489	220	130	1300	5000	<50	<50	<50	12000	<50	80	280	<50
Mn	80–4100	1433	815	10000	2000	7400	60	3000	<50	7000	<50	70000	74000	12000
Cu	<10–50	23	20	10	2	<5	8	13	<5	<5	6	<5	<5	190
Zn	30–620	171	50	55	180	79	6500	120	93	37	43	55000	57000	3800
Ba	<100–200	<100	<100	<100	19	27	20	19	25	25	19	15	17	22
Co	50–300	180	175	<50	30	180	130	100	100	190	120	610	620	380
Cr	<50	<50	<50	<50	<5	<5	<5	<5	<5	<5	<5	<5	<5	<5
Mo	<50–90	51	47	<50	42	64	7	46	28	37	12	5	<5	32
Ni	<50	<50	<50	<50	6	<5	42	6	<5	8	<5	490	530	5
Al	<50–120	48	<50	<50	<50	<50	1100	<50	<50	<50	<50	51000	52000	80
As	9–680	312	295	2000	340	450	10	69	13	780	41	<5	<5	40
Cd	<0.2–2.4	1	<0.2	<0.2	8.4	2.1	74	2.6	<0.5	<0.5	0.7	980	1000	65
Pb	<2–2	<2	<2	<2	<1	<5	<5	<5	<5	<5	<5	30	25	<5
Sb	<3–4	2	<3	<3	<3	7	5	6	6	<5	<5	<5	<5	<5
Li	<20	<20	<20	10	2.5	6	12	5	<5	<5	<5	46	43	6
Rb	90–470	303	355	160	<5	9	30	74	33	22	49	<5	BDL	45
U	<1–7.4	2	<1	1.2	20	<5	<5	10	<5	8	7	39	38	10

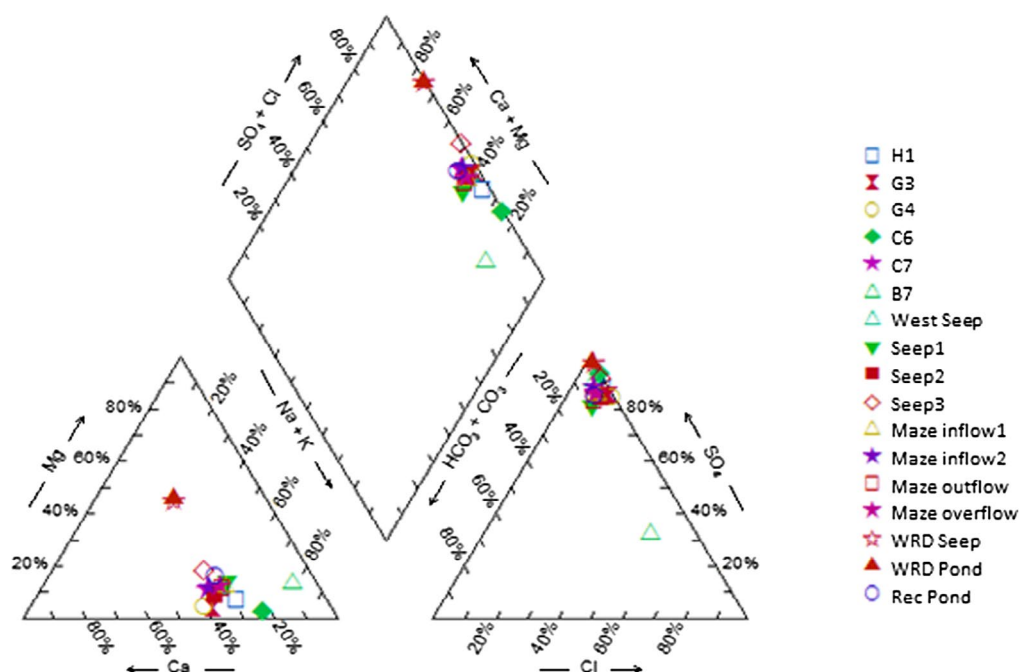


Figure 7. Piper diagram showing major cation and anion composition of water samples. Piezometers 1-6: H1, G3, G4, C6, C7, B7.

Seepage chemistry and passive treatment system

After passing through a 2.35 ha maze shape constructed wetland, the eastern seepage(s) from the TSF flow into the reclaim pond, where it mixes with seepage water from a waste rock dump (WRD). Because of the recent rise of water levels within the TSF in August 2008, it was possible to sample previously dry seepage points upstream from the wetland system (Figure 2).

Table 2 compares the chemistry of TSF seepage and piezometer water to those of waste rock seepages. The tailings seepages were Na-SO₄ water types with predominantly alkaline pH, a range of conductivities of 4900–5900 µS/cm and a sulphate range of 1700–2700 mg/L, whereas the WRD seepage was Mg-SO₄ type, acidic (pH 4.2) water, with higher conductivity (5700 µS/cm) and sulphate (3400 mg/L) at the source. At the reclaim pond, the combination of waters resulted in a pH of 7.7.

Figure 8 presents water quality trends for seepages from WRD and TSF and Figure 9 plots the data of the current study.

As would be expected from the slightly alkaline nature of the tailings seepage, the range of concentrations of metals including Al (0.050–1.1 mg/L), Mn (<0.05–10 mg/L), Zn (0.055–6.5 mg/L), Cd (0.008–0.074 mg/L), Cu (0.002–0.010 mg/L), Pb (<0.001 mg/L), Ni (<0.005–0.042 mg/L), U (<0.005–0.020 mg/L) and Co (0.050–0.180 mg/L) was much lower than those for the WRD seepage (see Figure 9). Kidston tailings contain carbonate minerals that were present in the gold deposit and CaCO₃ that was added to the cyanide-leaching circuit during gold extraction.

For the same reason, As (0.010–2 mg/L) and Mo (0.05–0.064 mg/L) concentrations in the TSF seepage were higher than those in the WRD seepage. Arsenic and Mo usually form oxyanions which are more mobile in high pH environments. Antimony, Se, Bi and Cu values were too close to detection limits to show a significant difference. TSF iron is in the range of <0.05–5 mg/L which is relatively high than the WRD seepage (0.28 mg/L). The lower concentrations of Fe in WRD seepage water could be explained by the oxidising conditions and formation of iron precipitates within WRD.

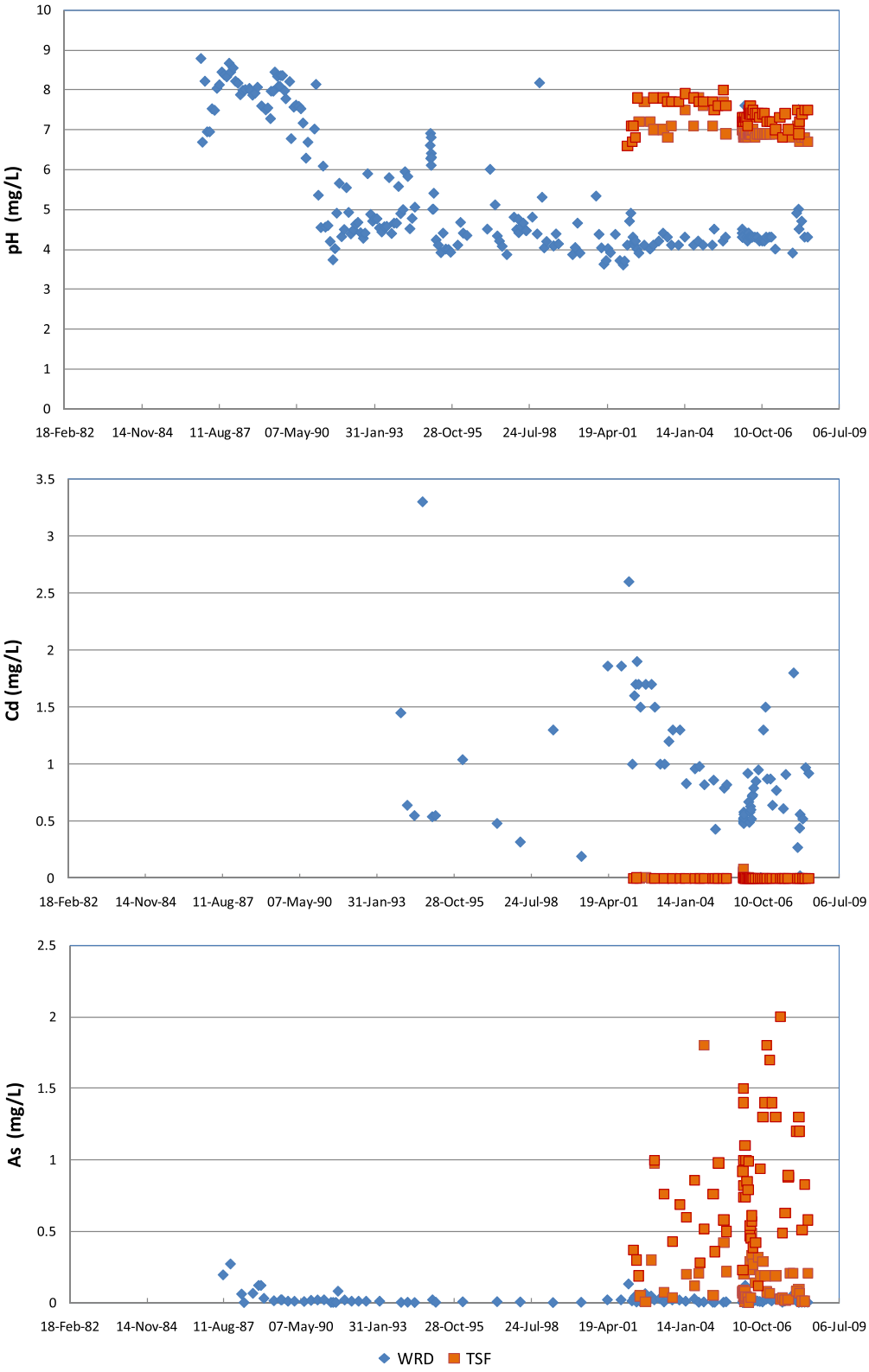


Figure 8. Plots of site water quality monitoring data comparing pH, Cd and As trends in the WRD and TSF seepages.

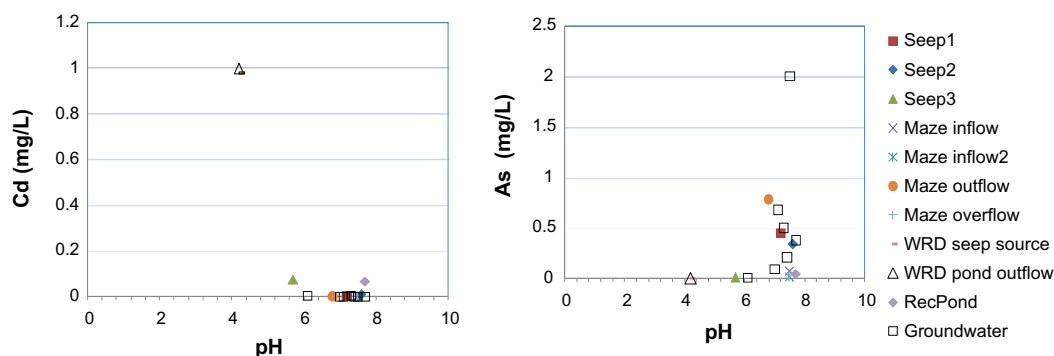


Figure 9. Plots of As and Cd concentrations vs pH in sampled waters from various sources.

One tailings seepage sample (Seep3) had exceptionally lower pH (5.7) and higher Mg, Al, Zn concentrations which are indicative of WRD seepage signatures and probably showed the influence of waste rocks in the structure of the TSF wall.

The chemistry of tailings seepages closely resembled those of piezometers. However, at the western seepage point the concentrations of arsenic were higher than those of piezometers and eastern seepages. Higher concentration of arsenic at this point could be related to higher concentrations of arsenopyrite in the western part of TSF or lesser chance of attenuation by secondary minerals, such as iron phases identified in the sequential extraction test and described by others [e.g. 26], due to lesser thickness of tailings.

A comparison of the water chemistry of inflow and outflow points of the constructed wetland at the primary seepage point of the TSF showed that while concentrations of dissolved sulphate remain relatively unchanged through the maze, concentrations of Fe (12 mg/L) increase substantially from inlet seepage points to the outflow point. Similarly, As (0.78 mg/L) and Mn (7 mg/L) concentrations are also higher at the outflow. Assuming the absence of hidden seepage points entering the maze, it may be concluded that the wetland system is inefficient and overly saturated resulting in the release of Fe and As.

Formation of abundant orange-brown Fe oxyhydroxides, identified as Ferrihydrite [$\text{Fe}_5\text{O}_7\text{OH}\cdot 5\text{H}_2\text{O}$] by XRD, at the outflow point of the wetland, indicates the change from reducing to oxidising conditions. The wetland maze floor was at least partly under reducing conditions as evidenced also by the H_2S odour. Under reducing conditions, the most common form of iron is Fe^{2+} which is much more soluble than Fe^{3+} . Formation of Fe precipitates and sorption properties is dependent on pH, residence time and redox-potential [27,28]. Ferrihydrite forms are oxidising near-neutral ($\text{pH} > 5.0$) environments. A fresh oxide surface has the capability to adsorb 10 times as much trace element as aged surfaces [29]. The sampled ferrihydrite at the maze outflow contained 3.2% Fe, 2.2% As, 42 mg/kg Mo, 37 mg/kg Pb, 1.5% Al, 2.7% Cu and 73 mg/kg Cu.

The wetland sediments contained high concentrations of C (28.2%) and N (1.19%) in the organic near surface fraction which is composed mainly of decaying litter, but also higher Al (2.3% average) and Fe (1.8% average) compared to those of 0.8% and 0.1%, respectively, for the detritus sediments below. The higher Fe and Al oxyhydroxides at the surface is common to wetlands used for mine drainage treatment [30]. The wetland sediments also comprised sulphides in localised anaerobic pockets with S concentrations in these locations varying from 1.5 to 2.9%.

Noller et al. [30] showed that decomposing surfaces of dead wetland plants provide adsorption sites, and at high pH, organic colloids have much higher cation exchange capacity (CEC) than inorganic colloids. In addition, Jain and Ram [31] stated that adsorption and complexation with humic and fluvic acids also play an important role in the sorption of metals by sediments. The organic fraction of the sediments contained up to 1742 mg/kg Cu, 80,453 mg/kg Mn, 527 mg/kg As and 215 mg/kg Cd.

The efflorescence salts collected around the wetland area were identified to be mainly bloedite $[(\text{Na}_2\text{Mg}(\text{SO}_4)_2 \cdot 4\text{H}_2\text{O})]$, with lesser amounts of halite (NaCl), gypsum (CaSO_4) and thenardite (Na_2SO_4). Mixing of circum-neutral TSF water and acidic WRD water resulted in light brown precipitates (or floc) in the bottom of the reclaim pond. The mineralogy of the floc consisted of gibbsite $[\text{Al}(\text{OH})_3]$ and some unidentified Al hydroxide minerals, and contained 6086 mg/kg Zn, 1843 mg/kg As and 28 mg/kg Cd.

Despite the presence of very high Cl and Na concentrations in plant tissues due to the dissolution and uptake of surface salts, the wetland plants have not accumulated detrimental levels of metals, consistent with relatively low concentrations of heavy metals in the tailings seepage water. The trace element concentrations for *Casuarina* sp. and *Melaleuca* sp. are in the range of 4.67–8.67 mg/kg Cu, 6.33–13.33 mg/kg As, 0–1.33 mg/kg Cd, 8.33–9.00 mg/kg Pb, 3.67–33.67 mg/kg Zn and 99–168.67 mg/kg Mn which are within the same range as those for *Typha* sp. with the exception of Mn (2191 mg/kg in *Typha* sp.). The current beneficial function of plants seems to be mainly limited to improving evapotranspiration and stabilisation of the wetland structure.

Conclusions

An understanding of the geochemistry, water chemistry and water balance within the TSF itself, combined with knowledge of the water chemistry of seepages of different origins and the chemistry of the resulting mixtures, provides a useful basis from which a more effective passive treatment system for seepage can be developed.

There were progressive dry areas of surface where the oxidation processes commenced and when the discharge of tailings into the TSF stopped, an unsaturated zone gradually formed and oxidation on the whole surface of the tailings started. Addition of alkaline substances to the tailings in the process plant, the presence of carbonate minerals and weathering of relatively fast weathering Mg-bearing minerals, chlorite and clays maintained the pH at a neutral to alkaline level, which encouraged the adsorption of liberated elements, thereby reducing the chances of their mobility. Near the surface of the TSF, secondary Fe(III) hydroxides precipitate *in situ* in the fine-grained horizons, where the main sulphide oxidation takes place. The sequential extraction showed the potential of these layers for adsorbing As which is mobile in the thermodynamic conditions of the tailings.

The knowledge of tailings horizons helps to make predictions of plant-available water, root proliferation capacity and potential accumulation of metals and metalloids in the above-ground biomass. While the accumulation of salts and Cd and Zn may not be as severe as in climatically dryer areas, it can, nonetheless, represent a local management challenge.

The rate of sulphide oxidation and natural attenuation of contaminants such as acidity and metal and metalloid ions within the TSF (or the balance between proton-producing and proton-consuming processes) will change over time, but the timing and the potential onset and duration of acid generation is unknown. Similar to some other tailings (e.g. see Ref. [32]), the combined effect of a slow moving oxidation front, sorption of heavy metals and metalloids in a large volume of non-weathered tailings and long transport times for dissolved ions in groundwater within the TSF may result in a time lag for release of contaminant-rich water of several decades. Further predictive modelling of the quality of leachate from the TSF requires detailed assessment of long-term sulphide oxidation by O_2 , as well as other geochemical processes that are slow and limited by (bio)geochemical kinetics, sulphide oxidation by Fe(III), oxidation of dissolved Fe(II) and aluminosilicate dissolution.

Elevated concentrations of arsenic recorded in tailings entrained water and at seepage points are attenuated by the presence of secondary minerals (iron oxides and hydroxides). One major outcome of this study was demonstrating the role of ferrihydrite in the attenuation of arsenic which showed dissolved arsenic was not dispersed far from the seepage points.

The practical outcome of the study, based on the element mobility in tailings, and the chemistry of seepage waters and precipitates, is that a combined passive treatment system including (1) an anaerobic wetland to remove sulphate and metals, and (2) an aerobic wetland to remove arsenic and

iron by oxidation seems to be an option that could improve the quality of seepage water from the tailings and WRDs. There is a cost benefit in mixing the seepages from tailings and waste rock as less alkalinity-producing material will be needed and the size of the anaerobic wetland can be reduced. However, formation of secondary minerals and floc such as Fe–Al and Mn-oxyhydroxides should be considered in the design of the treatment system because, as shown above, these secondary products cannot only act as sinks of trace elements, but also as potential sludge-forming materials.

Installation of deeper piezometers in the central area of the TSF, timely high-resolution data acquisition of the seepage rates and soil moisture measurements would greatly improve the understanding and response of the TSF water balance to changing environmental factors and may better define the role of vegetation in reducing seepage. Thereafter, the longevity of pyritic material in tailings can be more accurately calculated. Although geochemical modelling of the tailings groundwater showed that As and heavy metals could potentially remain mobile at lower depths of the TSF, knowledge of fluctuations of the water table and the geochemistry of deeper sections of tailings would help to better understand mechanisms that control the release and attenuation processes within TSF.

Acknowledgements

The authors gratefully acknowledge Genex Power for the review and approval of this paper. The base knowledge of the Kidston mine environment underlying the concepts presented in this paper is the result of a history of more than a decade of work by fellow researchers at the Centre for Mined Land Rehabilitation.

Disclosure statement

No potential conflict of interest was reported by the authors.

ORCID

Mansour Edraki  <http://orcid.org/0000-0002-9889-5716>

Thomas Baumgartl  <http://orcid.org/0000-0003-1613-7522>

Ali Munawar  <http://orcid.org/0000-0002-5731-8402>

References

- [1] G.E. Blight, *Erosion losses from the surfaces of gold-tailings dams*, J. South Afr. Inst. Mining Metall 89(1) (1989), pp. 23–29.
- [2] K.A. Mason, P.E.H. Gregg, and R.B. Stewart, *Land reclamation trials and practices at Martha Hill Gold Mine, Waihi, New Zealand*, Proceedings of the 1995 PACRIM Congress: Exploring the Rim, Auckland, New Zealand, 1995.
- [3] S.U. Salmon and M.E. Malström, *Geochemical processes in mill tailings deposits: modelling of groundwater composition*, Appl. Geochem. 19 (2004), pp. 1–17.
- [4] B. Dold and L. Fontboté, *Element cycling and secondary mineralogy in porphyry copper tailings as a function of climate, primary mineralogy, and mineral processing*, J. Geochem. Exploration 74(1–3) (2001), pp. 3–55.
- [5] B. Dold and L. Fontboté, *A mineralogical and geochemical study of element mobility in sulfide mine tailings of Fe oxide Cu–Au deposits from the Punta del Cobre Belt, northern Chile*, Chem. Geol. 189 (2002), pp. 3–4, 135–163.
- [6] M.C. Moncur, C.J. Ptacek, D.W. Blowes, and J.L. Jambor, *Release, transport and attenuation of metals from an old tailings impoundments*, Appl. Geochem. 20 (2005), pp. 639–659.
- [7] J. Smuda, B. Dold, J.E. Spangenberg, and H.-R. Pfeifer, *Geochemistry and stable isotope composition of fresh alkaline porphyry copper tailings: Implications on sources and mobility of elements during transport and early stages of deposition*, Chem. Geol. 256 (2008), pp. 62–76.
- [8] H. Holmström, U.J. Salmon, E. Carlsson, P. Paraskev, and B. Öhlander, *Geochemical investigation of sulfide-bearing tailings at Kristineberg, northern Sweden, a few years after remediation*, Sci. Total Environ. 273 (2001), pp. 111–133.
- [9] H. Holmström and B. Öhlander, *Layers in Fe- and Mn-oxyhydroxides formed at the tailings-pond water interface, a possible trap for trace metals in flooded mine tailings*, J. Geochem. Exploration 74 (2001), pp. 189–203.
- [10] B.G. Lottermoser, M.T. Costelloe, and P.M. Ashley, *Tailings dam seepage at the Rehabilitated Mary Kathleen Uranium mine, Northwest Queensland, Australia*, Proceedings of the 6th International Conference on Acid Rock Drainage, Cairns, 12–18 July 2003, pp. 733–738.

- [11] B.S. Gilfedder and B.G. Lottermoser, Biogeochemical evaluation of soil covers for base metal tailings, Ag-Pb-Zn Cannington mine, Australia, in *Geochemistry Research Advances*, Ólafur Strefánsson, ed., Nova Science Publishing Inc., New York, USA, **2008**, pp. 163–180.
- [12] P.M. Ashley, B.G. Lottermoser, A.J. Collins, and C.D. Grant, *Environmental geochemistry of the derelict Webs Consol mine, New South Wales, Australia*, Environ. Geol. **46** (**2004**), pp. 591–604.
- [13] H. Mustard, *Geology and genesis of the Kidston gold deposit, Australia*, in *Gold '86: An International Symposium on the Geology of Gold Deposits*, J.A. Maconald, ed., Toronto, **1986**, pp. 404–415.
- [14] D.J. Williams and N.A. Currey, *Engineering closure of an open pit gold operation in a semi-arid climate*, Int. J. Surf. Mining Reclam. Environ. **16**(4) (**2002**), pp. 270–288.
- [15] C.P. Horn, H.B. So, and D.R. Mulligan, *Waste rock dump rehabilitation research project – Stability of outer dump surfaces*, Progress Report No. 2., University of Queensland, **1998**.
- [16] Australasian Groundwater & Environmental Consultants Pty, Kidston tailings dam rehabilitation numerical model and water balance, **2001**, 26 pp.
- [17] D.J. Williams, D.R. Mulligan, and N.A. Currey. (**2006**). *A reflection and analysis of the waste rock dump closure strategies at Kidston Gold Mine*, in *First International Seminar on Mine Closure. First International Seminar on Mine Closure*, Perth, Western Australia, 13–15 September 2006, A. Fourie and M. Tibbett, eds., pp. 463–472.
- [18] N.V. Sidenko, E.I. Khozhina, and B.L. Sherriff, *The cycling of Ni, Zn, Cu in the system “mine tailings-groundwater-plants”: A case study*, Appl. Geochem. **22** (**2007**), pp. 30–52.
- [19] S.J. Roseby, P.M. Kopittke, D.R. Mulligan, and N.W. Menzies, *Evaluation of pyritic mine tailings as a plant growth substrate*, J. Environ. Manage. **201** (**2017**), pp. 207–214.
- [20] D.W. Rassam and D.J. Williams, *Engineering properties of gold tailings*, Int. J. Surf. Mining Reclam. Environ. **13**(3) (**1999**), pp. 91–96.
- [21] E.M. Baker and E.S. Andrew, *Geologic, fluid inclusion, and stable isotope studies of the gold-bearing breccia pipe at Kidston, Queensland, Australia*, Econ. Geol. **86** (**1991**), pp. 810–830.
- [22] E.M. Rykaart, *A methodology to describe spatial surface flux boundary conditions for solving tailings impoundment closure water balance problems*, PhD thesis, Department of Civil Engineering, University of Saskatchewan, Saskatoon, Canada, **2002**.
- [23] D.L. Parkhurst, *User's guide to PHREEQC—a computer program for speciation, reaction path. Advective transport and inverse geochemical calculations*. Water Resour. Invest. Rep. US Geol. Surv., Lakewood, Colorado, **1995**, pp. 95–4227.
- [24] J.W. Ball and D.K. Nordstrom, *User's manual for WATEQ4F, with revised thermodynamic database and test cases for calculating speciation of major, trace and redox elements in natural waters*, US Geol. Surv. Open-File Rep., **1991**, pp. 91–183. (Revised and reprinted August 1992).
- [25] D.K. Nordstrom and C.N. Alpers, *Geochemistry of acid mine waters*, in *The Environmental Geochemistry of Minerals Deposits. Reviews in Economic Geology*, G.S. Plumlee and M.J. Logsdon, eds., Soc. Econ. Geologists, Chelsea, MA, **1999**, pp. 133–160. (Chapter 6).
- [26] C. Casiot, M. Leblanc, O. Bruneel, J.-C. Personné, K. Koffi, and F. Elbaz-polichet, *Geochemical processes controlling formation of As-rich waters within a tailings impoundment (Carnoulès, France)*, Aquat. Geochem. **9** (**2003**), p. 237290.
- [27] G. Lee, J.M. Bigham, and G. Faure, *Removal of trace metals by coprecipitation with Fe, Al, and Mn from natural waters contaminated with acid mine drainage in the Ducktown Mining District, Tennessee*, Appl. Geochem. **17** (**2002**), pp. 569–581.
- [28] L.E. Schemel, B.A. Kimball, R.L. Runkel, and M.H. Cox, *Formation of mixed Al-Fe colloidal sorbent and dissolved-colloidal partitioning of Cu and Zn in the Cement Creek-Aminas River Confluence, Silverton, Colorado*, Appl. Geochem. **22** (**2007**), pp. 1467–1484.
- [29] J.M. Bigham and D.K. Nordstrom, *Iron and aluminium hydroxysulphates from acid sulfatewaters*, in *Sulfate Minerals, Crystallography, Geochemistry, and Environmental Significance. Reviews in Mineralogy and Geochemistry*, Vol. 40, C.N. Alpers, J.I. Jambor, and D.K. Nordstrom, eds., Mineralogical Society of America, Washington, DC, **2000**, pp. 351–403.
- [30] B.N. Noller, G.K. Parker, and G.H. Gao, *Metal and solute transportation through a wetland at a lead zinc mine, Northern Territory, Australia*. Eur. J. Mineral Process. Environ. Prot. **3**(1) (**2003**), pp. 15–35.
- [31] C.K. Jain and D. Ram, *Adsorption of metal ions on bed sediments*, Hydrol. Sci. J. **42**(5) (**1997**), pp. 713–723.
- [32] J. Ljungberg and B. Öhlander, *The geochemical dynamics of oxidising mine tailings at Laver, northern Sweden*, J. Geochem. Exploration **74** (**2001**), pp. 57–72.